Chemical-Kinetic Prediction
of Critical Parameters in Gaseous Detonations

Charles K. Westbrook
Paul A. Urtiew

MASTER

This paper was prepared for submittal to
the Nineteenth International Symposium on
Combustion, Haifa, Israel, August 8-13, 1982

January 12, 1982

Lawrence
Livermore
National
Laboratory

DISCLAIMER

DISCLAIMER

Portions of this document may be illegible in electronic image products. Images are produced from the best available original document.

Chemical-Kinetic Prediction of Critical Parameters

in Gaseous Detonations

Charles K. Westbrook   UCRL--87089

Paul A. Urtiew   DE82 007144

Lawrence Livermore National Laboratory
University of California
P.O. Box 808
Livermore, California 94550

Abstract

A theoretical model including a detailed chemical kinetic reaction

mechanism for hydrogen and hydrocarbon oxidation is used to examine the

effects of variations in initial pressure and temperature on the detonation

properties of gaseous fuel-oxidizer mixtures. Fuels considered include

hydrogen, methane, ethane, ethylene, and acetylene. Induction lengths are

computed for initial pressures between 0.01 and 10.0 atmospheres and initial

temperatures between 200K and 500K. These induction lengths are then

compared with available experimental data for critical energy and critical

tube diameter for initiation of spherical detonation, as well as detonation

limits in linear tubes. Combined with earlier studies concerning variations

in fuel-oxidizer equivalence ratio and degree of dilution with N_2, the

model provides a unified treatment of fuel oxidation kinetics in detonations.

INTRODUCTION

Gaseous detonations represent an important class of potential hazards associated with many industrial and energy production systems. Detonations have been studied experimentally for many years, but only recently have detailed theoretical and numerical treatments begun to appear. Although submodels for the fluid mechanics and other physical processes were developed rapidly; chemical kinetics submodels for the fuel combustion have been the weakest part of existing detonation models. However, current development of comprehensive kinetic reaction mechanisms for the oxidation of many practical fuels [1] has changed this situation significantly.

Recently we have shown [2,3] that it is possible to correlate many detonation parameters with chemical induction times, computed using a detailed kinetic mechanism. Experimental data for lean and rich limits for propagation of detonations in linear tubes, critical energy for initiation of unconfined spherical detonations, and critical tube diameters for initiation of unconfined spherical detonation by means of a planar detonation from a linear tube all were reproduced very well by the kinetic model. Fuels considered included methane (CH_4), ethane (C_2H_6), ethylene (C_2H_4), acetylene (C_2H_2), methanol (CH_3OH), and hydrogen (H_2), with oxidizers ranging from pure O_2 to air ($N_2/O_2 = 3.76$). However, only mixtures initially at atmospheric pressure and 300 K were examined. In the present study we extend this model to consider the effects of variations in initial pressure and temperature of the unreacted gas mixture, including pressures between 0.01 and 10 atmospheres, and temperatures from 200 to 500 K.

The success of the model at reproducing available experimental data suggests strongly that this technique provides a reliable basis for predicting detonation properties for conditions which have not yet been explored

experimentally. In particular, very few experimental data are available for detonation properties at initial pressures above 1 atm, at initial temperatures different from normal room temperature, or for mixtures in which the oxidizer is air rather than oxygen. The present model provides the best available means of estimating these properties.

CHEMICAL KINETICS

The chemical kinetic mechanism used for these computations has been developed and validated in a series of papers [4-7] and was used previously for modeling kinetics under detonation conditions [2,3]. The individual rate parameters can be found in References [2] and [7]. The mechanism has been shown to describe oxidation of methane [4,5], methanol [6], and ethylene [7] over wide ranges of experimental conditions. It has also been used to describe the shock tube oxidation of ethane [5,8] and acetylene [2], although truly comprehensive mechanisms for oxidation of these two fuels have not yet been developed. Since the parameter ranges in detonations are very similar to those encountered in laboratory shock tubes, it can be expected that the mechanism should provide reasonable results for ethane and acetylene oxidation in detonation waves.

The H_2 oxidation submechanism has been extensively validated, with nearly all of the elementary reaction rates being well established. As a result, computed induction times for H_2 oxidation are least likely to include significant kinetic errors. Disagreements between computed and experimental detonation parameters can be attributed to deficiencies in the overall physical model rather than to an inadequate kinetics model for H_2. Further discussion of the details of the kinetics model can be found in the references cited [2,7].

In the past, detonation models have used global rate expressions to complete chemical induction times for fuel-oxidizer mixtures, but such expressions are often not satisfactory, even when they have been based on shock tube data. Most shock tube experiments are carried out with high dilution by Ar, He, or N_2, so that fuel and oxygen concentrations are usually quite low. However, overall reaction order and effective activation energy in global expressions for induction time often change with the amount of dilution. These global rate parameters can also change significantly with pressure and temperature, especially in the case of H_2. As a result, induction times computed from global expressions can be seriously in error when applied to undiluted fuel-oxygen or fuel-air mixtures over wide ranges of equivalence ratio, initial pressure, or initial temperature, making a detailed kinetic mechanism an essential part of the present detonation model.

DETONATION MODEL

The model used here is the Zeldovich-von Neumann-Doring (ZND) model in which, locally, a detonation consists of a shock wave traveling at the Chapman-Jouguet (CJ) velocity, followed by a reaction zone. The shock wave compresses and heats the fuel-oxidizer mixture which then begins to react. In most mixtures, the fuel oxidation consists of a relatively long induction period during which the temperature and pressure remain nearly constant, followed by a rapid release of chemical energy and temperature increase.

For each fuel-oxidizer mixture, a calculation is first made of the relevant CJ conditions. From the resulting value of the detonation velocity D_{CJ}, the conditions in the von Neumann spike, including the temperature T_1, pressure P_1, and particle velocity v_1 of the post-shock, unreacted gases can be calculated and then used as initial conditions for the chemical

kinetics model. It is well established that the structure of the detonation wave is not one-dimensional but consists rather of a multidimensional conglomerate of individual cells. Furthermore, the shock velocity varies within a single detonation cell from an initial value of about 1.6 D_{CJ} to a minimum of about 0.6 D_{CJ}, so the CJ conditions used here represent average values, and the computed induction times will also be averages.

The reactive mixture is assumed to remain at a constant volume over its reaction time, and the induction time is defined in terms of its temperature history. Most of the mixtures examined underwent a large temperature increase of 1000 - 2000 K, and the induction time is defined as the time of maximum rate of temperature increase. In most cases, this coincides approximately with the time at which the temperature has completed about half of its total increase. This is not, strictly speaking, a true induction period, often defined as the time required for a small (i.e., 1 - 5%) temperature or pressure increase, but it represents a time scale for the release of a significant amount of energy. In addition to the induction time τ, it is useful to define the induction length $\Delta \equiv \tau(D_{CJ} - v_1)$.

As a result of these simplifications, the computed induction times and induction lengths define characteristic time and length scales rather than a precise history of a gas element through the detonation front. The evolution of the reacted gas subsequent to the induction period considered here is dominated by the fluid mechanics of the post-induction expansion of the reaction products. This expansion reduces both the pressure and density of these products and alters the kinetic equilibrium state, leading eventually to the final CJ state. The present model does not attempt to follow that entire relaxation phase, concentrating on the details of the induction processes in the von Neumann spike.

Although this model is a simple one and neglects some potentially significant effects arising from hydrodynamic-kinetic interactions, it has been very successful at modeling detonation parameters with fuel-oxidizer mixtures initially at atmospheric pressure and 300 K. With the same reaction mechanism as that used for the present study, it was shown [2,3] that the computed induction length Δ is proportional to the critical tube diameter d_c for initiation of unconfined spherical detonation. For all the fuels examined and with oxidizers ranging from O_2 (i.e., $\beta = N_2/O_2 = 0$) to air ($\beta = 3.76$), the expression

$$d_c = 380 \, \Delta \qquad (1)$$

accurately reproduced experimental data for d_c from a variety of sources [9-11]. In Fig. 1 the variation of Δ with N_2 dilution is summarized for stoichiometric fuel-O_2-N_2 mixtures, initially at atmospheric pressure and 300 K. Experimental data from Ref. [9] for fuel-O_2 conditions (i.e., $\beta = 0$) are also indicated and the agreement between computed and measured results is quite close. Similar agreement was obtained at other values of β and fuel-oxidizer equivalence ratio [2,3]. The fact that a single scaling exists between Δ and d_c for all of the fuels examined, indicates that the model can be used to predict values of d_c for other mixtures, at other initial conditions, and for other related fuels. In addition, it was shown that the cube of the induction length Δ^3 correlates closely with the critical energy required for initiation of unconfined spherical detonation, with initiation by means of either high explosive charges or a planar detonation from a linear tube.

For the case of initiation of spherical detonation by means of a linear tube, Lee et al. [9,12] have developed an expression for E_c based on the concept of the work needed to produce a sufficiently strong initiation source in the unconfined gas. Urtiew and Tarver [13] used a similar approach to show that the critical energy is related to the critical tube diameter through the expression

$$E_c = k_0 \frac{Pu}{D} d_c^3 \qquad (2)$$

where pressure P and particle velocity u are those of the CJ state behind the detonation wave in the tube.

When Eqs. (1) and (2) are combined, the resulting expression

$$E_c = k_0 \frac{Pu}{D} (380)^3 \Delta^3 \qquad (3)$$

relates E_c to the computed induction length and CJ parameters of a particular mixture. As the equivalence ratio is varied for hydrocarbon fuels and for hydrogen, the quantity $(Pu/D) \Delta^3$ is in fairly good agreement with the values of E_c deduced by Matsui and Lee [9] from their experimental values of d_c. This is shown in Fig. 2 which includes only the results pertaining to fuel-oxygen mixtures. For k_0 in Eq. (3), the value 0.1964 derived theoretically by Urtiew and Tarver [13] has been used. Again, it is possible to conclude that a single scaling law applies to all of the fuel-O_2 mixtures, this time over a wide range of equivalence ratio.

EFFECTS OF PRESSURE

For each stoichiometric fuel-oxidizer mixture, CJ and induction time calculations were carried out over a range of inital pressures P_o between 0.01 and 10 atm. The computed values of induction length are summarized in Fig. 3. For all of the hydrocarbon-O_2 mixtures, P_o can be expressed in terms of Δ by a straight line

$$P_o = k_1 \, \Delta^{-\alpha} \, . \tag{4}$$

Combining this with Eq. (1) gives the expression

$$P_o = k_2 \, d_c^{-\alpha} . \tag{5}$$

The constants k_1, k_2 and α depend on the type of fuel. Also shown in Fig. 3 are experimental results [9] relating d_c and P_o. The scales for d_c and Δ have been set in accordance with Eq. (1). For a given tube of diameter d_c and a specified fuel-oxidizer mixture, it is observed that below the critical pressure indicated by the dotted line in Fig. 3, the linear detonation will not initiate an unconfined spherical detonation. For all of the hydrocarbon-O_2 fuels the agreement between the computed solid curves and the experimental dotted lines is very good, indicating that Eq. (1) remains valid when P_o is varied, and that for those fuel-O_2 mixtures Eq. (5) is a reasonable means of relating P_o and d_c. The kinetic model results in Fig. 3 for $H_2 + \frac{1}{2} O_2$ appear slightly curved, although the straight line representing the data of Matsui and Lee agrees very well with the computed results over the range of pressures studied.

Computed values of Δ for stoichoimetric fuel-air mixtures are also shown in Fig. 3. For these mixtures, only the results for C_2H_6-air fall along a straight line. The most surprising behavior is that of stoichiometric H_2-air, which has multiple values of P_0 for a range of d_c between 9 and 15 cm. Computed results for the other mixtures are also somewhat curved, with methane once again being an exception with the curvature in the opposite direction. However, none of the hydrocarbon-air mixtures show the multiple-valued behavior displayed by H_2-air.

The computed results for H_2-air are caused by the gradual growth in importance of the recombination reaction $H + O_2 + M = HO_2 + M$ with increasing pressure. In this way the behavior is reminiscent of the second explosion limit for H_2-O_2 described by Lewis and von Elbe [14]. The rate of this reaction is pressure-dependent, and as the post-shock unreacted gas pressure increases it eventually begins to compete with the principal chain branching reaction $H + O_2 = O + OH$. When this occurs the overall rate of fuel consumption actually decreases as P_0 increases, due to the reduced chain branching rate, so the induction length grows larger. Further increases in P_0 reverse this trend and Δ again decreases with increasing P_0. This second reversal occurs because the greater density and species concentrations provide more rapid rates of the key bimolecular reactions which overcome the inhibiting effect of the recombination reaction. In particular, the HO_2 thus formed is rapidly consumed by the sequence of reactions

$$HO_2 + HO_2 = H_2O_2 + O_2$$
$$H_2O_2 + M = OH + OH + M$$
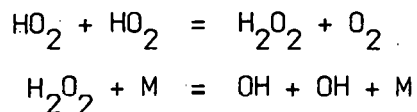
making this effectively a chain propagation path.

Of the fuel-air mixtures, experimental data for the reaction of d_c with P_0 could be found only for C_2H_2 [9]. For this case the computed results also agree well with the measured data. Bull et al. [15] measured the detonation cell length a in H_2-air at initial pressures below atmospheric, finding a distinct discontinuity in the graph of log a versus log P_0. This discontinuity, occurring at $P_0 \simeq 0.15$ atm, was attributed to a change in the dominant kinetic processes which govern the cell spacing, consisting of recombination processes at very low pressures and induction kinetics at higher pressures [16]. In Fig. 3 there is no discontinuity at $P_0 \simeq 0.15$ atm for H_2-air, suggesting that Δ may not necessarily be proportional to the cell length at low pressures, particularly if the kinetics are so slow that the induction phase is not nearly complete within the von Neumann spike. There is evidently a need for experimental measurement of the dependence of critical tube diameters on pressure in fuel-air mixtures, including measurements for initial pressures in excess of 1 atm, in order to verify the predictions indicated in Fig. 3. The curvature shown for many of the fuels suggests that Eq. (5) can be expected to be reliable only over limited ranges of pressure. In particular, the unexpected variation of d_c with initial pressure for H_2-air requires further attention. The numerical predictions suggest that H_2-air at high initial pressures will require significantly larger critical tube diameters to initiate unconfined spherical detonations than would be predicted on the basis of extrapolated low pressure experiments. This may have important consequences in assessing potential hazards associated with H_2-air mixtures.

Matsui and Lee [9] define the relative detonation hazard D_H as the ratio of the critical energy E_c for initiation of unconfined spherical detonation for a given mixture to that for a reference mixture, $C_2H_2+1.5O_2$. Both E_c and D_H were computed at several values of P_o for the fuel-O_2 and fuel-air mixtures included in this study, using Eq. (3). The results are summarized in Table I. The computed reference value of E_c for $C_2H_2+1.5O_2$ is 4.54×10^{-4} joules, close to the value of 3.83×10^{-4} joules derived by Matsui and Lee from their measurements of d_c. For those gases where the pressure dependence of Δ can be described adequately by Eq. (4), the exponent α is about equal to 1. Combined with Eqs. (1) and (2), this results in

$$E_c \sim P_o^{-2} . \qquad (6)$$

However, the deviation from this trend for H_2-air at high pressure is large. Based on Eq. (6) and the low pressure H_2-air values for Δ, D_H at $P_o = 10$ atm would be approximately equal to 9.37×10^2, rather than the value of 3.45×10^6 actually predicted by the detailed kinetic model. For all of the fuel-air mixtures, and for the fuel-O_2 mixtures outside the ranges examined experimentally, the present model provides the only available means of estimating those detonation parameters.

EFFECTS OF TEMPERATURE

An additional series of CJ and induction time calculations was carried out with the initial gas temperature varied from 200 K to 500 K. All of the fuel-O_2 and fuel-air mixtures were stoichiometric, and the initial pressure P_o was assumed to be atmospheric. The computed results for Δ are summarized in Fig. 4 and Table I.

In every case, as the initial temperature T_0 is increased, the induction length also increases. This is due to two factors both related to the conditions behind the unreacted shock. Most important, because the initial pressure P_0 is constant, the post-shock density ρ_1 decreases with increasing T_0. Most of the elementary chemical reactions are bimolecular, with rates that vary with ρ^2, so as T_0 increases and ρ_1 decreases, the overall rate of reaction is reduced. Second, the post-shock unreacted temperature T_1, which is used to initiate the kinetics calculations, actually decreases slightly with increasing values of T_0. For example, for C_2H_4-air, T_1 = 1555 K when T_0 = 200 K, while T_1 = 1470 K when T_0 = 500 K. The combination of lower post-shock temperature and lower reactant concentrations results in larger induction times as T_0 increases.

As seen in Fig. 4, the relative ranking among the fuels in terms of induction length remains nearly constant as T_0 varies. At $T_0 \simeq 375$ K, the values of Δ for H_2-air and C_2H_2-air are approximately equal, and for higher temperatures H_2-air is actually slightly more detonable, but the values of Δ for the two fuels remain very similar. Methane-air mixtures are affected most by increases in T_0, but qualitatively the behavior of all of the fuel-oxidizer mixtures to variations in T_0 is the same.

It has been observed both experimentally and in modeling studies [5, 17-19] that although the induction time for CH_4-air mixtures is much larger than for other alkane fuels, the addition of relatively small quantities of H_2, C_2H_6, C_3H_8, or other hydrocarbons can reduce the induction time dramatically. Liquefied natural gas (LNG) consists of approximately 90% CH_4 with the remainder made up of C_2H_6, C_3H_8, and other trace constituents. When CJ and induction length calculations were carried out for

a stoichiometric fuel-air mixture, with the fuel consisting of 90% CH_4 and 10% C_2H_6, this kinetic sensitization was observed at all values of T_0 considered. The dependence of Δ on T_0 for this LNG-like fuel is indicated in Fig. 4 and can be seen to be the same as that of the single component fuels.

The magnitude of the change in induction length over temperature ranges which might occur in actual spills of liquefied gaseous fuels such as LNG can be seen to be quite small, but it should not be neglected. For example, LNG is stored at about 110 K, so a stoichiometric LNG-air mixture resulting from a spill would have an initial temperature of about 275 K rather than 300 K. The induction length at T_0 = 275 K is 1.03 x 10^{-2} m, 15% smaller than the computed value Δ = 1.21 x 10^{-2} m at T_0 = 300 K. In addition to a slight increase in detonability limits, this 15% reduction in Δ would also result in a 40% reduction in Δ^3. As pointed out earlier, the critical energy of initiation E_c is proportional to Δ^3 for unconfined spherical detonation. Therefore, a gas mixture initially at 275 K would require a substantially smaller energy for initiation of detonation than a mixture at 300 K.

SUMMARY

Chemical kinetics of fuel oxidation plays a key role in the initiation and propagation of detonation waves. In earlier studies we demonstrated that it is possible to relate computed chemical kinetic induction times and induction lengths to a variety of critical detonation parameters for fuel-oxidizer mixtures which are initially at atmospheric pressure and 300 K. In the present paper we have shown that the same approach can be extended to include a wide range of initial pressure and temperature as well. For

conditions in which experimental data are available,* the agreement between computed and measured results is excellent. Under conditions where experimental data are unavailable and difficult or impossible to obtain, the present model provides a means of estimating these detonation parameters.

This model is intentionally oversimplified in order to emphasize the purely kinetic factors involved in detonation phenomena. A complete model of detonations, their initiation, propagation and stability will require a much more sophisticated fluid mechanics submodel and probably require a two-dimensional or even three-dimensional treatment, well beyond the goals and capabilities of the present work. However, the kinetic model alone has been shown to provide a great deal of useful information and can be used in many cases to interpret existing experimental data or predict detonation parameters which have not been measured. This type of kinetics modeling is very simple and inexpensive to carry out, using any of a large number of computer programs which are capable of integrating stiff kinetics equations. In addition, the present study shows that the description of the kinetics of fuel oxidation is no longer the weak link in our understanding of detonation phenomena.

REFERENCES

1. Westbrook, C.K., and Dryer, F.L., Eighteenth Symposium (International) on Combustion, p. 749, The Combustion Institute, Pittsburgh, 1981.

2. Westbrook, C.K., Chemical kinetics of hydrocarbon oxidation in gaseous detonations, Combustion and Flame, in press (1982).

3. Westbrook, C.K., Hydrogen oxidation kinetics in gaseous detonations, submitted for publication (1982).

4. Westbrook, C.K., Creighton, J., Lund, C., and Dryer, F.L., J. Phys. Chem. 81, 2542 (1977).

5. Westbrook, C.K., Combust. Sci. and Technol. 20, 5 (1979).

6. Westbrook, C.K., and Dryer, F.L., Combust. Sci. and Technol. 20, 125 (1979).

7. Westbrook, C.K., Dryer, F.L., and Schug, K.P., A comprehensive mechanism for the pyrolysis and oxidation of ethylene, submitted for publication (1982).

8. Westbrook, C.K., and Haselman, L.C., Progress in Aeronautics and Astronautics, vol. 75, p. 193 (1981).

9. Matsui, H., and Lee, J.H., Seventeenth Symposium (International) on Combustion, p. 1269, The Combustion Institute, Pittsburgh, 1979.

10. Moen, I.O., Donato, M., Knystautas, R., and Lee, J.H., Eighteenth Symposium (International) on Combustion, p. 1615, The Combustion Institute, Pittsburgh, 1981.

11. Zeldovich, Y.B., Kogarko, S.M., and Semenov, N.N., Soviet Phys. Tech. Phys. 1, 1689 (1956).

12. Lee, J.H., and Matsui, H., Combustion and Flame 28, 61 (1977).

13. Urtiew, P.A., and Tarver, C.M., Progress in Aeronautics and Astronautics, vol. 75, p. 370, 1981.

14. Lewis, B., and von Elbe, G., Combustion, Flames and Explosions of Gases, Academic Press, New York (1961).

15. Bull, D.C., Elsworth, J.E., Shuff, P.J., and Metcalfe, E., submitted to Combustion and Flame.

16. Edwards, D.H., Hooper, G., Job, E.M., and Parry, D.J., Astronautica Acta 15, 323 (1970).

17. Crossley, R.W., Dorko, E.A., Scheller, K. and Burcat, A., Combustion and Flame <u>19</u>, 373 (1972).

18. Bull, D.C., Ellsworth, J.E., and Hooper, G., Combustion and Flame <u>34</u>, 327 (1979).

19. Eubank, C.S. Rabinowitz, M.J., Gardiner, W.C., Jr., and Zellner, R.E., Eighteenth Symposium (International) on Combustion, p. 1767, The Combustion Institute, Pittsburgh, 1981.

Table I

Selected critical parameters for fuel-air and fuel-oxygen mixtures.
Values of E_C can be obtained by multiplying D_H by 4.54×10^{-4} J.
Numbers inside parentheses indicate powers of 10.

P_0 (atm)	T_0 (K)	fuel-air				fuel-oxygen			
		τ (μs)	Δ (m)	d_C (m)	D_H	τ (μs)	Δ (m)	d_C (m)	D_H
H_2									
.01	300	1.80(+2)	6.35(-2)	2.41(+1)	3.78(10)	3.50(+1)	1.72(-2)	6.54(00)	8.90(+8)
.10	300	8.10(00)	2.92(-3)	1.11(00)	3.81(+7)	1.40(00)	7.01(-4)	2.66(-1)	6.53(+5)
1.0	300	8.00(-1)	2.87(-4)	1.10(-1)	3.72(+5)	8.80(-2)	4.49(-5)	1.71(-2)	1.86(+3)
10.	300	7.50(-1)	2.78(-4)	1.10(-1)	3.45(+6)	1.40(-2)	7.39(-6)	2.81(-3)	1.64(+2)
1.0	200	5.50(-1)	1.99(-4)	8.00(-2)	1.92(+5)	5.40(-2)	2.79(-5)	1.06(-2)	6.91(+2)
1.0	500	1.54(00)	5.36(-4)	2.00(-1)	1.37(+6)	1.82(-1)	8.99(-5)	3.42(-2)	8.44(+3)
C_2H_2									
.01	300	9.50(+1)	2.76(-2)	1.05(+1)	3.77(+9)	3.60(00)	9.72(-4)	3.69(-1)	2.84(+5)
.10	300	7.60(00)	2.24(-3)	8.50(-1)	2.11(+7)	2.40(-1)	6.67(-5)	2.53(-2)	1.00(+3)
1.0	300	9.10(-1)	2.73(-4)	1.00(-1)	3.96(+5)	1.70(-2)	4.83(-6)	1.84(-3)	4.17(00)
10.	300	1.23(-1)	3.70(-5)	1.00(-2)	1.02(+4)	1.30(-3)	3.86(-7)	1.47(-4)	2.34(-2)
1.0	200	6.00(-1)	1.78(-4)	7.00(-2)	1.60(+5)	9.76(-3)	2.88(-6)	1.09(-3)	1.35(00)
1.0	500	2.10(00)	5.89(-4)	2.20(-1)	2.10(+6)	3.47(-2)	9.72(-6)	3.69(-3)	1.95(+1)
C_2H_4									
.01	300	1.07(+3)	2.99(-1)	1.14(+2)	4.66(12)	3.40(+1)	4.21(-3)	1.60(00)	2.34(+7)
.10	300	7.10(+1)	2.01(-2)	7.64(00)	1.47(10)	1.78(00)	3.42(-4)	1.30(-1)	1.36(+5)
1.0	300	8.90(00)	2.56(-3)	9.70(-1)	3.12(+8)	1.10(-1)	2.82(-5)	1.07(-2)	8.26(+2)
10.	300	1.45(00)	4.26(-4)	1.60(-1)	1.48(+7)	9.40(-3)	2.25(-6)	8.55(-4)	4.39(00)
1.0	200	5.67(00)	1.67(-3)	6.30(-1)	1.33(+8)	6.70(-2)	1.73(-5)	6.57(-3)	2.93(+2)
1.0	500	1.98(+1)	5.50(-3)	2.09(00)	1.77(+9)	2.30(-1)	5.73(-5)	2.18(-2)	3.99(+3)
C_2H_6									
.01	300	7.70(+2)	2.10(-1)	7.98(+1)	1.59(12)	1.60(+1)	3.62(-3)	1.38(00)	1.53(+7)
.10	300	1.05(+2)	2.90(-2)	1.10(+1)	4.33(10)	1.50(00)	3.47(-4)	1.32(-1)	1.45(+5)
1.0	300	1.62(+1)	4.55(-3)	1.73(00)	1.64(+9)	1.60(-1)	3.78(-5)	1.44(-2)	2.03(+3)
10.	300	2.50(00)	7.13(-4)	2.70(-1)	6.72(+7)	1.56(-2)	3.76(-6)	1.43(-3)	2.16(+1)
1.0	200	1.09(+1)	3.05(-3)	1.16(00)	8.10(+8)	7.76(-2)	2.29(-5)	8.70(-3)	6.80(+2)
1.0	500	3.57(+1)	1.00(-2)	3.80(00)	1.06(10)	2.84(-1)	7.94(-5)	3.02(-2)	1.06(+4)
CH_4									
.01	300	1.83(+4)	5.23(00)	1.99(+3)	2.35(16)	1.60(+2)	4.32(-2)	1.64(+1)	2.24(10)
.10	300	1.35(+3)	3.87(-1)	1.47(+2)	9.81(13)	9.12(00)	2.50(-3)	9.50(-1)	4.69(+7)
1.0	300	8.65(+1)	2.53(-2)	9.61(00)	2.80(11)	4.80(-1)	1.33(-4)	5.05(-2)	7.62(+4)
10.	300	3.92(00)	1.16(-3)	4.40(-1)	2.72(+8)	2.10(-2)	5.91(-6)	2.25(-3)	7.23(+1)
1.0	200	4.31(+1)	1.27(-2)	4.83(00)	5.45(10)	2.72(-1)	7.62(-5)	2.90(-2)	2.20(+4)
1.0	500	2.50(+2)	7.03(-2)	2.67(+1)	3.42(12)	1.11(00)	3.01(-4)	1.14(-1)	5.08(+5)

FIGURE CAPTIONS

1. Variation of computed induction length with N_2 dilution $(\beta=N_2/O_2)$
    for stoichiometric fuel-oxidizer mixtures. Initial pressure is one
    atmosphere.

2. Critical energy for initiation of unconfined sperical detonation. Open
    symbols represent results of Matsui and Lee [9], curves are computed from
    Eq. 3 with $k_o = 0.1964$.

3. Variation of computed length Δ and experimentally determined critical
    tube diameter d_c with P_o. Solid curves are computed results for
    fuel-O_2 mixtures, dashed curves for fuel-air mixtures, and dotted lines
    represent experimental data from reference [9].

4. Variation of induction length Δ with T_o. Solid lines represent
    fuel-O_2 mixtures, dashed curves represent fuel-air mixtures. The fuel
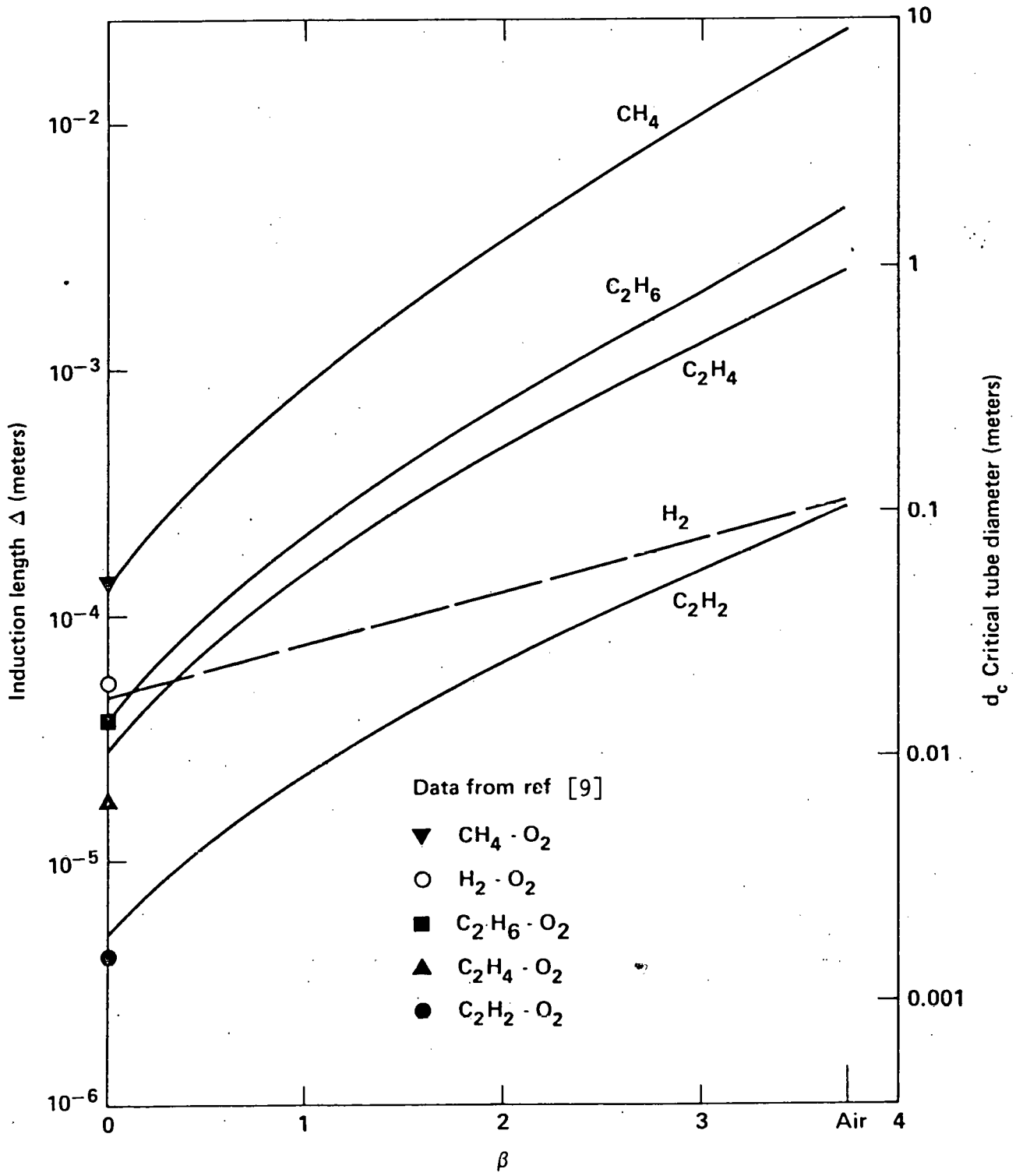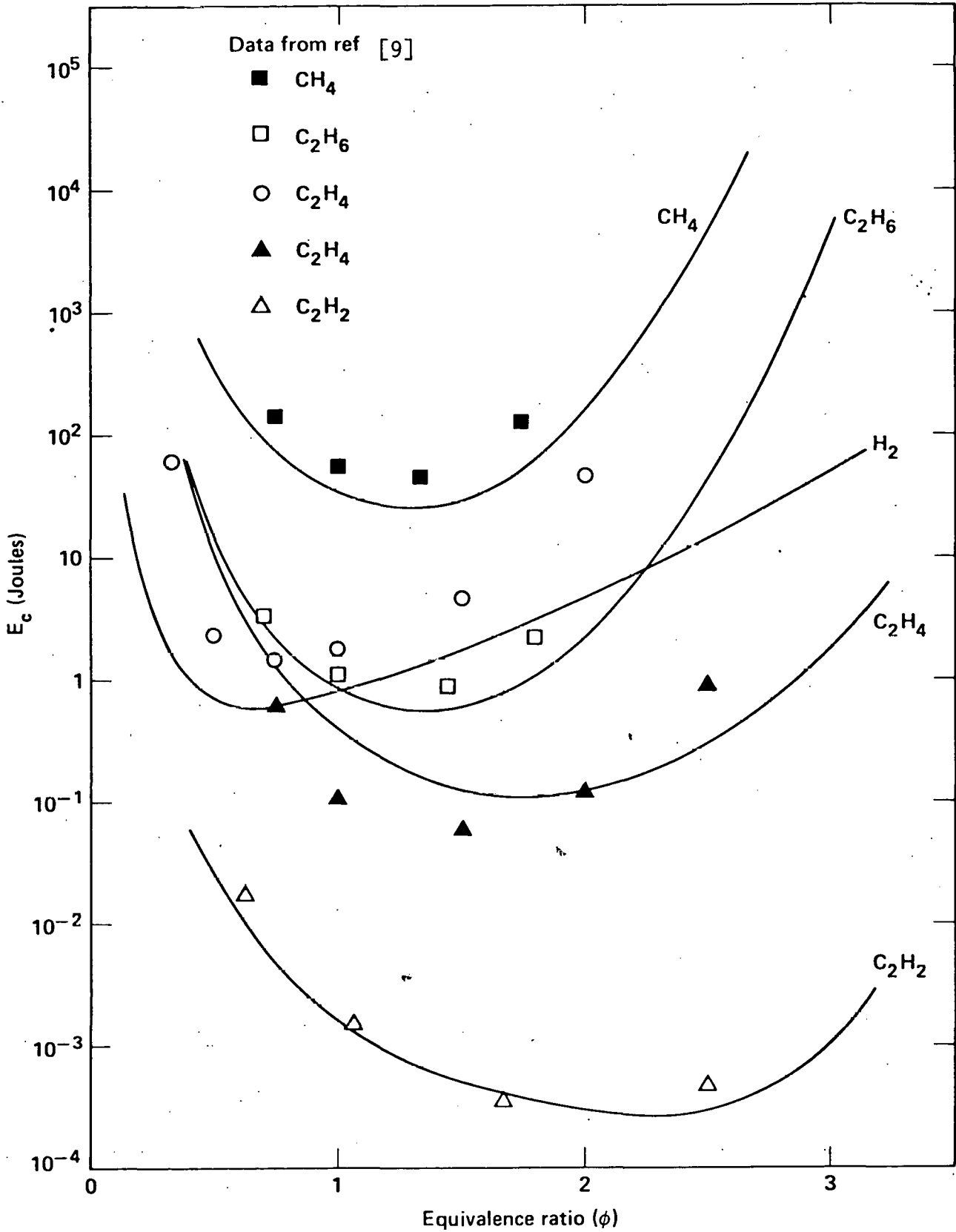   for the dashed curve labeled "LNG" consists of 90% CH_4 - 10% C_2H_6.
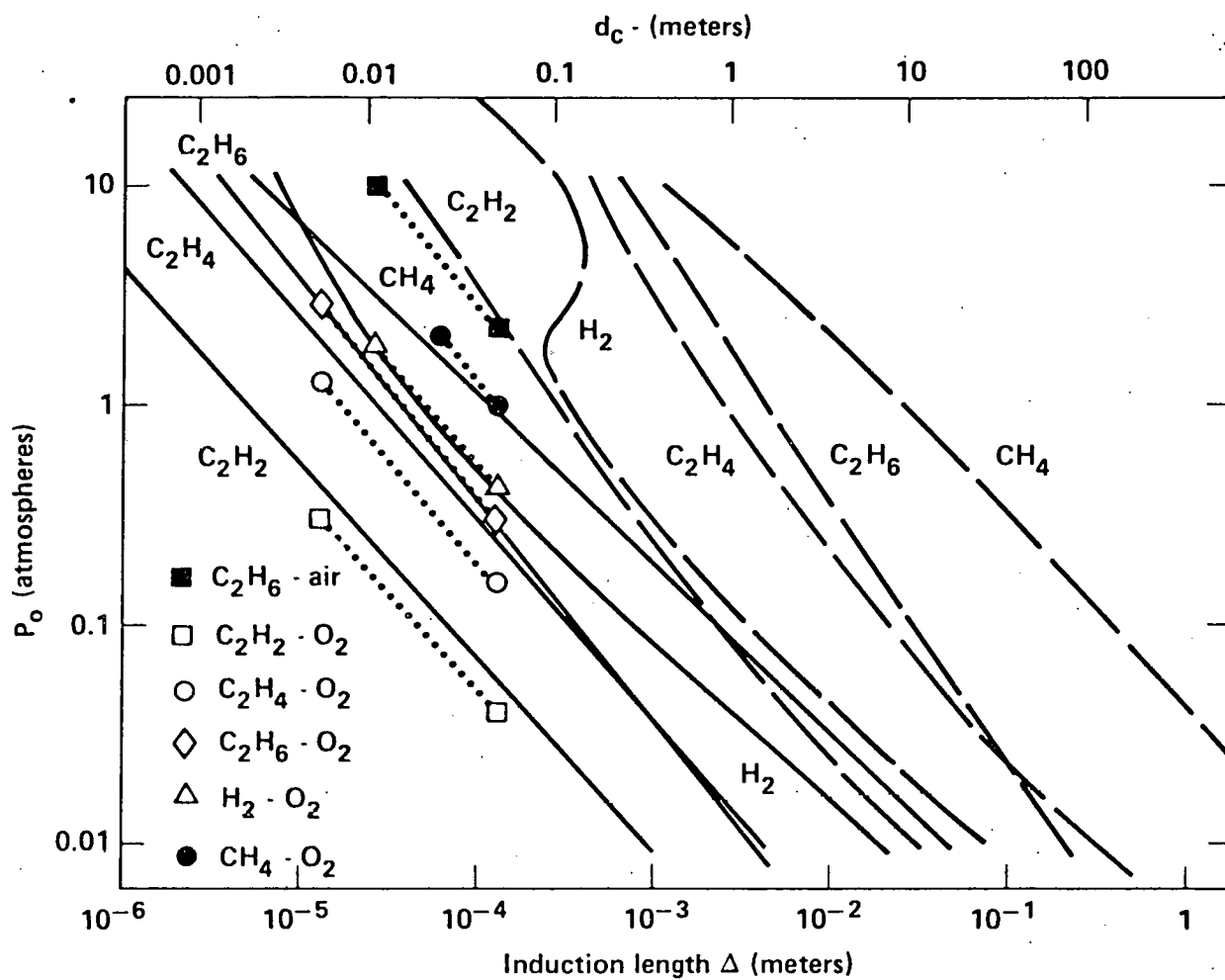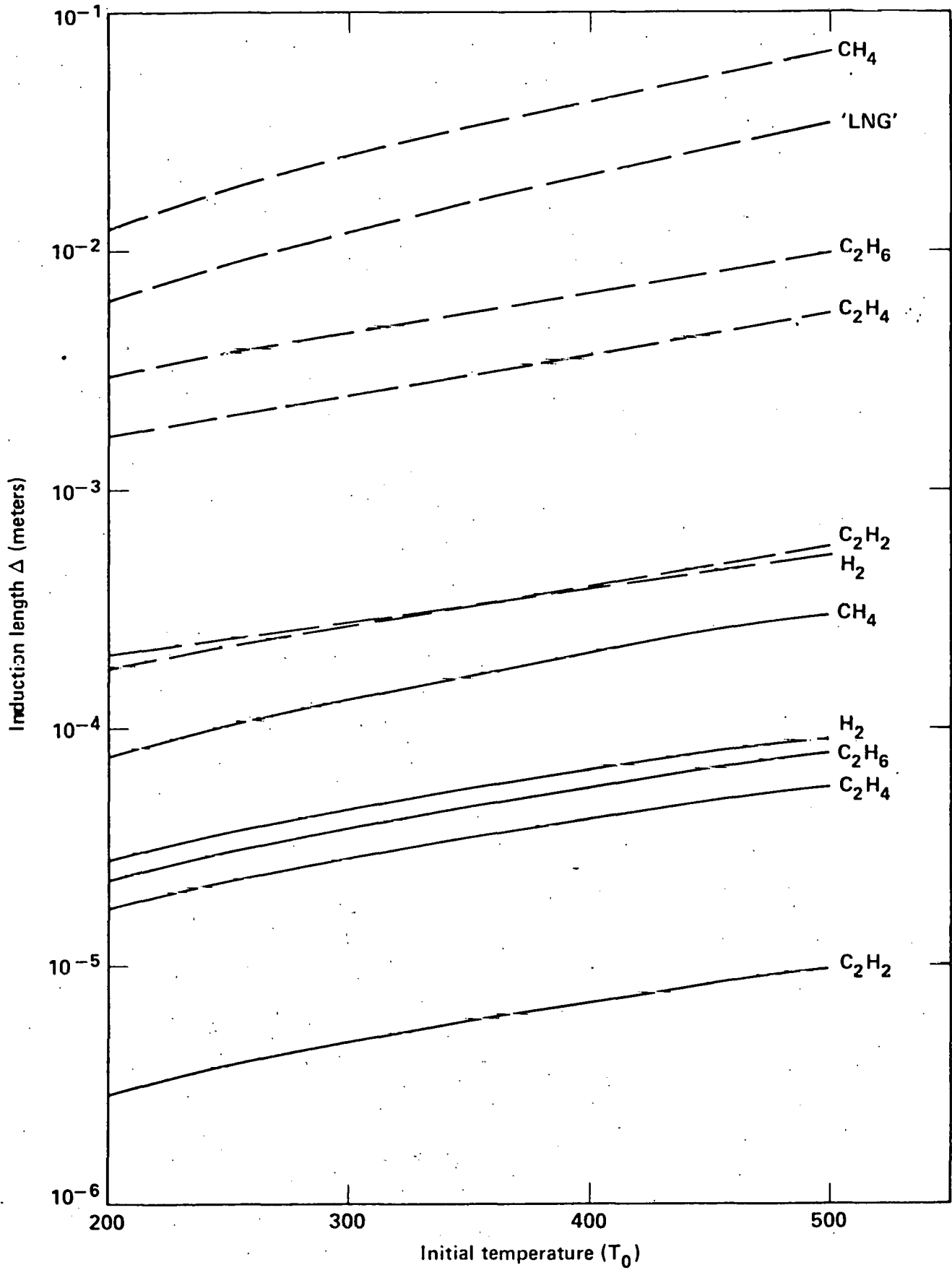
Figure 1

Figure 2

Figure 3

Figure 4